Scanning tunneling microscopy of an interfacial two-dimensional electron gas in oxide heterostructures

Igor Altfeder, Hyungwoo Lee, Jianjun Hu, Rachel D. Naguy, Alp Sehirlioglu, Amber N. Reed, Andrey A. Voevodin, and Chang-Beom Eom

Phys. Rev. B **93**, 115437 — Published 25 March 2016

DOI: 10.1103/PhysRevB.93.115437

Scanning Tunneling Microscopy of Interfacial Two Dimensional Electron Gas in Oxide Heterostructures

Igor Altfeder[1*], Hyungwoo Lee[2], Jianjun Hu[1], Rachel D. Naguy[1], Alp Sehirlioglu[3], Amber N. Reed[1], Andrey A. Voevodin[1] and Chang-Beom Eom[2]

[1]Nanoelectronic Materials Branch, Air Force Research Laboratory, Wright Patterson AFB, OH 45433, USA

[2]Department of Materials Science and Engineering, University of Wisconsin–Madison, Madison, WI 53706, USA

[3]Department of Materials Science and Engineering, Case Western Reserve University, Cleveland, OH 44106, USA

Using advanced technique combining pulsed laser deposition growth of $LaAlO_3$, $LaTiO_3$ and $SrTiO_3$ we effectively constructed half-integer unit cell number $LaAlO_3$-$SrTiO_3$ heterostructures where all interfaces are of LaO-TiO_2 type, and two dimensional electron gas (2DEG) forms symmetric n-type bilayer. Using ultra high vacuum scanning tunneling microscopy we investigated the properties of surface 2DEG in these heterostructures. Our results indicate that surface 2DEG is strongly, within one unit cell, confined at the interface. Tunneling spectroscopy of surface 2DEG reveals thickness dependent band gap changes attributed to quantum size effect.

PACS: 73.20.-r, 68.37.Ef, 81.15.Fg

I. INTRODUCTION

Atomic layer controlled deposition of epitaxial heterostructures has resulted in significant advances in the growth of superlattices [1] and quantum wells [2]. The interfaces in these artificial structures have an important role in enabling and determining novel material functionalities and novel device applications. An interesting example of such novel interface-induced functionalities is the formation of two-dimensional electron gas (2DEG) at the interface of complex oxides $LaAlO_3$ (LAO) and $SrTiO_3$ (STO) [3]. In these heterostructures the 2DEG can be confined within several unit cells near the interface [4, 5]. Physically important ground states (magnetic and superconducting) of this 2DEG have been suggested and experimentally demonstrated [6-8], and critical applications in field-effect transistors have been proposed [9].

Several theoretical models have been proposed explaining different mechanisms contributing to formation of this 2DEG [4, 5, 10, 11] including: electrostatic doping produced by interfaces and doping induced by oxygen vacancies. The theoretical proposals of multiple LAO/STO-based 2DEG heterostructures have also been presented in the literature [4, 12]. The interest to multiple 2DEG heterostructures is stimulated by their potential applications in electronic devices including high-power electronic devices. According to these theoretical proposals [12], when LAO layer contains integer or half-integer unit cell (uc) number (see Figs. 1ab) the 2DEGs developing at its opposite sides have either opposite (n-type vs. p-type) or same carrier types, respectively. In the Figs. 1a and 1b, we show atomic layer structures for two basic types of such multiple-2DEG systems. While the "asymmetric" heterostructures, corresponding to Fig. 1a, have been already produced and experimentally studied [13, 14], growth of "symmetric" heterostructures requires solving a challenge of controlled half-integer uc number deposition. An interesting approach for design of such "symmetric" heterostructures is inserting

a single uc of $LaTiO_3$ (LTO) into the oxide matrix using pulsed laser deposition (PLD) technique [15]. As we show in the Fig. 1b, inserting a single uc of LTO indeed makes the heterostructure symmetric: both interfaces here are of LaO-TiO_2 type, and according to theory [4, 12] there have to be two symmetric n-type 2DEGs inside of such heterostructures, a buried 2DEG below LAO film and a surface 2DEG on top of LAO film. The formation of surface 2DEG makes these heterostructures an interesting system for scanning tunneling microscopy (STM) studies. Unlike the buried 2DEG that was extensively studied in earlier STM works [16, 17], the surface 2DEG will be extremely sensitive to environment. For example, it is anticipated that the electronic structure can be modified by adsorbed molecules, charge transfers to these molecules, contamination induced surface states, and Fermi level pinning at these surface states. Please note that while both n-type 2DEGs in such symmetric heterostructures are being affected by interfacial doping, the detailed physical mechanisms of such doping (for Fig. 1b case) may be different. Whereas the buried 2DEG is attributed to LAO-STO interfacial polarization [4, 5], the formation of surface 2DEG may be additionally enhanced by LTO-induced doping. In the bulk form LTO is known to be Mott-Hubbard insulator with correlation gap of ~0.2 eV [18]. The earlier studies of LTO-incorporating oxide interfaces [18, 19] considered LTO acting as a dopant layer due to the constituent T^{3+} ions, whose $3d^1$ electrons can "migrate" into the empty $3d^0$ orbitals in the STO.

In this manuscript, we present the first STM study of symmetric n-type 2DEG bilayer heterostructure grown by PLD. Our results confirm the formation of n-type surface 2DEG strongly confined at the interface, and whose formation most likely occurs due to interfacial doping mechanisms. We also report, for the first time, STM observation of band gap "blue shift" in ultra-thin STO capping layers, attributed to quantum size effect.

II. EXPERIMENT

The heterostructures were grown in an epitaxial PLD chamber equipped with differentially pumped reflective high energy electron diffraction (RHEED) gun for layer-by-layer monitoring and controlling the sample growth. The substrate was undoped (001)-oriented STO. The substrate temperature during PLD deposition was 800°C. The oxygen pressures during the sample growth were: a) 10^{-3} Torr for growth of 10 uc of LAO, b) 5×10^{-6} Torr for growth of 1 uc of LTO, and c) 10^{-2} Torr for growth of 3 uc of STO capping layer. Using very low oxygen pressure in case of LTO is required because another material phase ($La_2Ti_2O_7$ rather than $LaTiO_3$) grows in an oxygen reach environment [20]. High oxygen pressure for growth of STO capping layer was selected in order to eliminate oxygen vacancies in this layer. The thickness of LAO layer (10 uc) was chosen to at least by a factor of two exceed the critical thickness for formation of 2DEG in single-interface heterostructures, which is known to be 4 uc [3-5, 16, 17]. After accomplishment of PLD growth and extracting the samples from the PLD chamber, the interfaces were directly observed using high-resolution transmission electron microscope (TEM) (see Fig. 2a), and the atomically flat surface geometry of heterostructures was confirmed using ambient atomic force microscopy (AFM) (see Fig. 2b). The samples were then loaded into UHV chamber equipped with: variable-temperature scanning tunneling microscope from RHK Technology (model UHV300), in-situ heating stage for sample bakeout, and in-situ contacts for direct monitoring of surface electrical conductivity. The contacts were thin tantalum foils mechanically clamped to the surfaces of studied samples (see Fig. 2c). The initial surface resistance was >100 GΩ, the same "infinite" value that we saw just before loading the samples. We attribute this to contamination induced electronic structure changes possibly affecting not only the topmost layer in the studied heterostructures. The samples were then *in-situ* annealed to

350°C for 12 hours. The annealing temperature was chosen to efficiently outgas the adsorbed molecules from STO surface, but to prevent spontaneous formation of oxygen vacancies. The earlier studies have shown that formation of oxygen vacancies on STO surface requires annealing to significantly higher temperatures (>640ºC) [21, 22] compared to annealing temperatures that were used in our study (see also the Discussion part). The annealing was performed in a sequence of 3 hour long steps. After each of these annealing steps the sample was allowed to cool down to room temperature, and its electrical resistance was measured. The room temperature surface resistance decreased continuously, and finally reached a value of $\approx 2\times10^5$ Ω [23]. For reference, typical reported 2DEG room temperature sheet resistances for LAO/STO interfaces grown under similar conditions are in the range $10^4 - 10^5$ Ω [24, 25]. In order to additionally verify surface 2D nature of observed conductivity, the measurements were also performed on PLD grown LAO/STO samples (10 uc LAO) without the STO-LTO capping layer, using the same method of mechanically clamped Ta foils [26]. For these uncapped samples electrical conductivity was not observed both before and after UHV annealing.

The presence of n-type surface 2DEG was confirmed by STM measurements performed after UHV annealing. The STM measurements were performed at room temperature, using commercial Pt-Ir tip (from Bruker Corp.) that was *in-situ* cleaned by electron beam heating. In the Fig. 3a we show the 200×200 nm^2 STM image of the sample surface obtained after restoring surface 2DEG. The image was obtained at 30 pA tunneling current and 2.5 V sample bias. The STM image reveals atomically flat terraces and additional isolated STO islands having typical size and typical lateral separation of ~ 100 Å. The lateral cross section of the STM image, shown in the Fig. 3b, indicates that the height of these islands is 4 Å, which corresponds to STO uc height (a = 3.9 Å). These observations confirm that PLD growth of STO capping layer occurs by

whole unit cells rather than by individual TiO_2 and SrO atomic layers. From the Fig. 3a we also conclude that the islands cover 40% of the surface area. The ultrathin ("graphene-like") geometry of STO capping layer and the presence of islands makes these heterostructures an interesting model system for study of quantum confinement effects, such as band gap vs. thickness dependence.

In the Fig. 4a we show the typical tunneling current-voltage characteristic measured on top of STO island. The tunneling band gap of 3.9 eV and significant n-type asymmetry can be easily observed on this data after logarithmic linearization of the tunneling I-V curve [27], as shown in the inset of Fig. 4a (solid circles). Such processing of the I-V curve is usually a necessary step because it eliminates the exponential increase of tunneling current at large bias values [27, 28]. The positions of valence band maxima (VBM) and conduction band minima (CBM) are indicated by vertical arrows. The measured band gap value is significantly larger than the bulk band gap in STO crystals E_0 = 3.2 eV [29]. We attribute this to quantum size effect (QSE) [28, 30]. To verify this hypothesis a similar measurement was performed between the islands, where STO thickness is 3 rather than 4 unit cells. This measurement revealed an additional 0.1 eV increase of CBM position and 0.5 eV decrease of VBM position, as we also show in the inset of Fig. 4a (empty circles), altogether indicating 0.6 eV increase of the tunneling band gap. The band gap increase occurs due to formation of electronic subbands produced by QSE. The lowest unoccupied and the highest occupied subbands are the easiest for experimental detection, because only these subbands are directly involved in the apparent increase of the tunneling band gap. As it was earlier shown [27, 28], observation of detailed structure of QSE subbands on tunneling I-V curves is possible only under special conditions and requires (a) cryogenic temperatures, (b) ideal reflection conditions, and (c) significant out-of-plane vs. in-

plane effective mass anisotropy facilitating formation of narrow resonance-like subbands. These criteria are apparently not satisfied for reported here experimental setup, which explains why the subbands are not resolvable. Estimated from the tight binding model increase of the tunneling band gap due to contribution of lowest unoccupied and highest occupied subbands is given by

$$\Delta E_g \approx U_0 \left(1 - cos\frac{\pi}{n+1}\right) \quad (1)$$

where U_0 represents the average width of conduction and valence bands in the perpendicular to interface direction, n is the number of unit cells, and the "n+1" correction from the tight binding model was described in Ref. [28]. For studied here STO films ΔE_g is indeed anticipated to be ~1 eV [29]. In the Fig. 4b, the experimental data are compared to band gap vs. thickness dependence expected from Eq. (1) for U_0 = 4 eV, and excellent agreement is observed. Besides electron interference, other contributions to QSE may arise from size-dependent interactions in thin films. For example, confinement induced increase of band gaps was reported for van der Waals coupled layered 2D semiconductors [31], where interlayer electron transport is usually not considered as ballistic.

III. DISCUSSION

The earlier transport measurements on LTO doped interfaces [18, 32, 33] revealed the two-carrier nature of 2DEG in such heterostructures. It has been shown that 2DEG at LTO doped interfaces represents a mixture of strongly-confined (confined within 1-2 uc) and weekly-confined (confined within 5-10 nm) components [18, 32, 33]. Interestingly, the incomplete band bending observed by tunneling spectroscopy on STO capping layers (Fig. 4a) may indicate that surface 2DEG in our samples is strongly confined at the interface, i.e. confined within 1 uc. The Fig. 5a illustrates band bending in STO capping layer corresponding to this situation. According to Fig. 5a, tunneling measurements on top of STO capping layers reveal n-type "echo" of

strongly-confined 2DEG. Upon decreasing the thickness of STO capping layer the average band gap position shifts towards lower energies, in accordance with Fig. 5a prediction. Thus, our studies did not reveal weakly-confined 2DEG component. It seems likely that weakly-confined 2DEG component has been caused by oxygen vacancies, not present at the surfaces of studied here samples. The observed Arrhenius type decrease of resistance in 300–650 K range (Fig. 5b) [23], with activation energy close to 0.2 eV, indicates that Mott-Hubbard gap is preserved in LTO layers [18]. In Ref. [20] metallic carrier density in epitaxial 40–100 uc thick LTO layers has been reported and attributed to suppression of Mott-Hubbard gap due to strain caused by STO substrate. In our samples the epitaxial strains are anticipated to be comparable, and in a view of our new results it seems likely that reported in Ref. [20] effects could be caused by other mechanisms. In particular, those effects could be caused by strain-relaxation, expected to occur for 40–100 uc thickness range, accompanied by formation of LTO dislocations possibly responsible for observed there LTO metallicity.

Our interpretation of surface conductivity recovery as a result of annealing induced desorption seems rather natural for 350°C annealing process used in our study. Indeed, surface desorption energies are usually significantly lower than energies required for oxide unit cell decomposition. The first process is usually accompanied by breaking of van der Waals bonds between the adsorbed molecules and the sample surface, whereas the second process requires breaking of covalent bonds inside unit cell. For example, for typical CO desorption energy of 0.4 eV [34] and oxygen vacancy formation energy at STO surface of 4.87 eV (8 eV for bulk STO) [35], the rates ratio for these two processes would be $\sim 10^{31}$. The evidence of anomalous buildup of surface Ti^{3+} states in 250°C UHV annealed STO crystals has been reported in Ref. [36] and attributed to surface oxygen vacancy segregation [37, 38]. On surfaces of our samples, the

vacancy segregation mechanism unlikely takes place because of the presence of two interfacial diffusion barriers produced by LAO film. Besides, our results indicate that surface 2DEG is strongly confined at STO-LTO interface, and LTO Mott-Hubbard gap manifests in transport measurements [23], which makes even less likely the possibility of oxygen vacancy contribution to observed effects (although it cannot be completely ruled out). The comparison of STO-LTO capped and uncapped PLD grown samples shows that our simple contact preparation technique is sufficient for contacting 2DEG through 3-4 uc of STO, and prevents contacting another, significantly deeper located, interfacial 2DEG. The described in this work realization of multiple n-type 2DEG heterostructures, based on LTO uc incorporation, is not the only possible; other realization methods, based on multistage LAO-STO deposition have been described earlier [39].

IV. CONCLUSIONS

In conclusion, using innovative materials design approach we have constructed symmetric heterostructures in LAO/STO oxide matrix and experimentally observed tunneling into surface 2DEG. Our results suggest that interface induced doping is most likely responsible for formation of surface 2DEG. The ability to design and grow heterostructures with atomic-scale precision, to bring 2DEG to the surfaces of studied samples and to directly perform tunneling measurements on this 2DEG certainly opens new experimental pathway for studies of quantum effects in ultrathin films of semiconductors and physically important ground states of interfacial 2DEG, and for understanding its performance at the nanoscale for field-effect transistor applications.

ACKNOWLEDGMENTS

The authors acknowledge N. Zhitenev, K. Matveev, N. Bristowe, A. Roy, J. Wohlwend, A. Safriet, A. Crespo, and D. L. Dorsey for interesting discussions. The research is supported by AFOSR.

References

* e-mail Igor.Altfeder.Ctr@us.af.mil

1. R. People, J. C. Bean, D. V. Lang, A. M. Sergent, H. L. Störmer, K. W. Wecht, R. T. Lynch, and K. Baldwin, Appl. Phys. Lett. 45, 1231 (1984)

2. L. Goldstein, F. Glas, J. Y. Marzin, M. N. Charasse and G. Le Roux, Appl. Phys. Lett. 47, 1099 (1985)

3. A. Ohtomo and H. Y. Hwang, Nature 427, 423 (2004)

4. J. Lee and A. A. Demkov, Phys. Rev. B 78, 193104 (2008)

5. J. Gonjakowski, F. Finocchi, and C. Noguera, Rep. Prog. Phys. 71, 016501 (2008)

6. F. Bi, M. Huang, S. Ryu, H. Lee, C. W. Bark, C. B. Eom, P. Irvin, J. Levy, Nature Comm. 5, 5019 (2014)

7. M. Gabay and J. M. Triscone, Nature Physics 9, 610 (2013)

8. N. Reyren et al., Science 317, 1196 (2007)

9. M. Hosoda, Y. Hikita, H. Y. Hwang and C. Bell, Appl. Phys. Lett. 103, 103507 (2013)

10. J. N. Eckstein, Nature Materials 6, 473 (2007)

11. R. Pentcheva1 and W. E. Pickett, Phys. Rev. Lett. 102, 107602 (2009)

12. A. Janotti, L. Bjaalie, L. Gordon, and C. G. Van de Walle, Phys. Rev. B 86, 241108R (2012)

13. R. Pentcheva et al., Phys. Rev. Lett. 104, 166804 (2010)

14. M. Huijben, G. Rijnders, D. H. A. Blank, S. Bals, S. Van Aert, J. Verbeeck, G. Van Tendeloo, A. Brinkman, and H. Hilgenkamp, Nature Materials 5, 556 (2006)

15. H. W. Jang et al., Science 331, 886 (2011)

16. B. C. Huang et al., Phys. Rev. Lett. 109, 246807 (2012)

17. Z. Ristic, R. Di Capua, G. M. De Luca, F. Chiarella, G. Ghiringhelli, J. C. Cezar, N. B. Brookes, C. Richter, J. Mannhart, and M. Salluzzo, Europhys. Lett. 93, 17004 (2011)

18. M. Hosoda, C. Bell, Y. Hikita and H. Y. Hwang, Appl. Phys. Lett. 102, 091601 (2013)

19. S. Nazir, C. Bernal, K. Yang, ACS Appl. Mater. Interfaces 11, 5305 (2015)

20. F. J. Wong, S. H. Baek, R. V. Chopdekar, V. V. Mehta, H. W. Jang, C. B. Eom, and Y. Suzuki, Phys. Rev. B 81, 161101R (2010)

21. V. E. Henrich, G. Dresselhaus, H. J. Zeiger, Phys. Rev. B 17, 4908 (1978)

22. M. S. Martín González, M. H. Aguirre, E. Morán, M. Á. Alario-Franco, V. Perez-Dieste, J. Avila, and M. C. Asensio, Solid State Sci. 2, 519 (2000)

23. Post-annealing resistance vs. temperature measurements performed in 300–650 K range revealed Arrhenius type dependence (thermally activated transport) with activation energy of ≈0.2 eV (LTO Mott-Hubbard gap), indicating that some Mott-Hubbard character remains in LTO layer, as was also discussed in Ref. [18]. From these data, the contact induced resistance contribution was estimated to be < 5 kΩ.

24. J. W. Park et al., Nature Comm. 1, 94 (2010)

25. C. Li, Z. Liu, W. Lü, X. R. Wang, A. Annadi, Z. Huang, S. Zeng, Ariando, and T. Venkatesan, Sci. Rep. 5, 13314 (2015)

26. Making contacts to buried 2DEG was possible using another method of ultrasonically welded Al wires. Also, in some instances it was possible to contact buried 2DEG by applying voltage (~15 V) pulses to Ta contacts and inducing dielectric breakdown in LAO layer. The typical room temperature resistance of buried 2DEG (including contacts) was ~20 kΩ. The tunneling leakage through 10 uc LAO layer was estimated to be < 1 $G\Omega^{-1}/cm^2$.

27. I. B. Altfeder, X. Liang, T. Yamada, D. M. Chen, and V. Narayanamurti, Phys. Rev. Lett. 92, 226404 (2004)

28. I. B. Altfeder, K. A. Matveev, D. M. Chen, Phys. Rev. Lett. 78, 2815 (1997)

29. S. Piskunov, E. Heifets, R. I. Eglitis, G. Borstel, Comp. Mat. Sci. 29, 165 (2004)

30. A. D. Yoffe, Advances in Physics 51, 799 (2002)

31. K. F. Mak, C. Lee, J. Hone, J. Shan, and T. F. Heinz, Phys. Rev. Lett. 105, 136805 (2010)

32. R. Ohtsuka, M. Matvejeff, K. Nishio, R. Takahashi, and M. Lippmaa, Appl. Phys. Lett. 96, 192111 (2010)

33. J. Biscaras, N. Bergeal, S. Hurand, C. Grossetête, A. Rastogi, R. C. Budhani, D. LeBoeuf, C. Proust, and J. Lesueur, Phys. Rev. Lett. 108, 247004 (2012)

34. S. Azad, M. H. Engelhard, and L. Q. Wang, Journal of Physical Chemistry B 109, 10327 (2005)

35. V. E. Alexandrov, E. A. Kotomin, J. Maier, and R. A. Evarestov, Eur. Phys. J. B 72, 53 (2009)

36. R. Di Capua et al., Phys. Rev. B 86, 155425 (2012)

37. W. Sitaputra, N. Sivadas, M. Skowronski, D. Xiao, and R. M. Feenstra, Phys. Rev. B 91, 205408 (2015)

38. L. B. Xiong, J. L. Li, B. Yang and Y. Yu, Journal of Nanomaterials 2012, 831524 (2012)

39. H. J. Harsan Ma, Z. Huang, W. M. Lü, A. Annadi, S. W. Zeng, L. M. Wong, S. J. Wang, T. Venkatesan, and Ariando, Appl. Phys. Lett. 105, 011603 (2014)

Figure Captions

Figure 1 (color online)

a. Atomic layer structure for asymmetric 2DEG bilayer heterostructure. The AlO_2 layers are negatively charged, whereas the LaO layers are positively charged. Subsurface 2DEG is n-type, surface 2DEG is p-type.

b. Atomic layer structure for symmetric 2DEG bilayer heterostructure studied in this work. In this heterostructure both subsurface and surface 2DEGs are n-type. Symmetrization is achieved by deposition of single unit cell of LTO.

Figure 2 (color online)

a. High resolution TEM image of 2DEG bilayer heterostructure grown by PLD method. Before TEM measurements, the surface of heterostructure (the upper side of the image) was coated with amorphous carbon.

b. Ambient AFM image measured after removing the sample from the PLD chamber.

c. Schematics of UHV STM experimental setup. For STM measurements the bias potential was applied to sample contacts, and the STM tip was used to measure the current. To avoid the back-gating effect, during STM measurements the top and the bottom 2DEGs were electrically connected to each other [26].

Figure 3 (color online)

a. The 200×200 nm^2 STM image obtained after final UHV annealing of the sample. The image was obtained at 30 pA tunneling current and 2.5 V sample bias.

b. The lateral cross section of the STM image in Fig. a.

Figure 4 (color online)

a. Tunneling I-V curve measured on top of STO island after final UHV annealing of the sample. The horizontal axis shows sample bias (sample-to-tip bias).

Inset: (Solid circles) The same I-V curve after logarithmic linearization shows the asymmetric tunneling band gap characteristic for n-type doping. Solid arrows indicate the locations of valence band maxima (VBM) and conduction band minima (CBM). (Empty circles) Similar tunneling measurement performed between STO islands revealed larger band gap value. The VBM and CBM for this curve are indicated by dotted arrows. For both curves, the logarithmic linearization [27] uses function $arcsinh(I/I_0)$ with I_0 = 0.3 pA.

b. Comparison of experimental data (circles) and anticipated from QSE band gap vs. thickness dependence (diamonds). Bulk band gap is shown as dashed horizontal line.

Figure 5 (color online)

a. Illustration of electronic band bending above LAO film in STO-LTO capped sample. Tunneling measurements on top of STO capping layers reveal n-type "echo" of strongly confined at the interface 2DEG. Please note that STO thickness change from 4 to 3 uc (25%) is anticipated to shift both CBM and VBM positions towards lower energies. However, the corresponding band gap changes induced by QSE are more significant, resulting in CBM instead shifting towards higher energies.

b. Thermally activated transport revealed by post-annealing resistance vs. temperature measurements in 300–650 K range. The activation energy is close to 0.2 eV, i.e. LTO Mott-Hubbard gap.

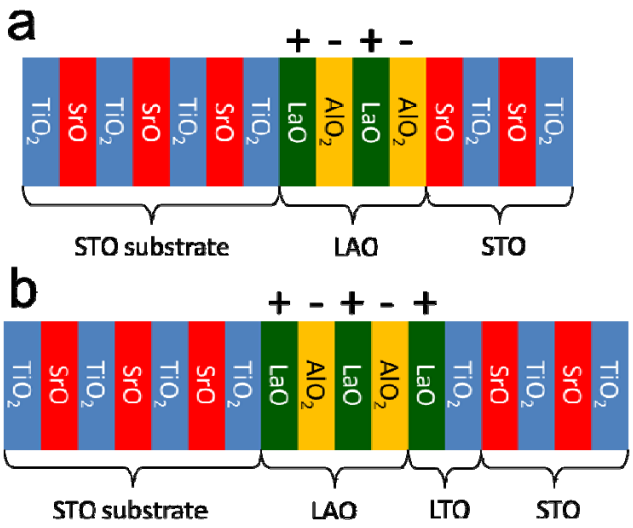

Altfeder et al. Figure 1

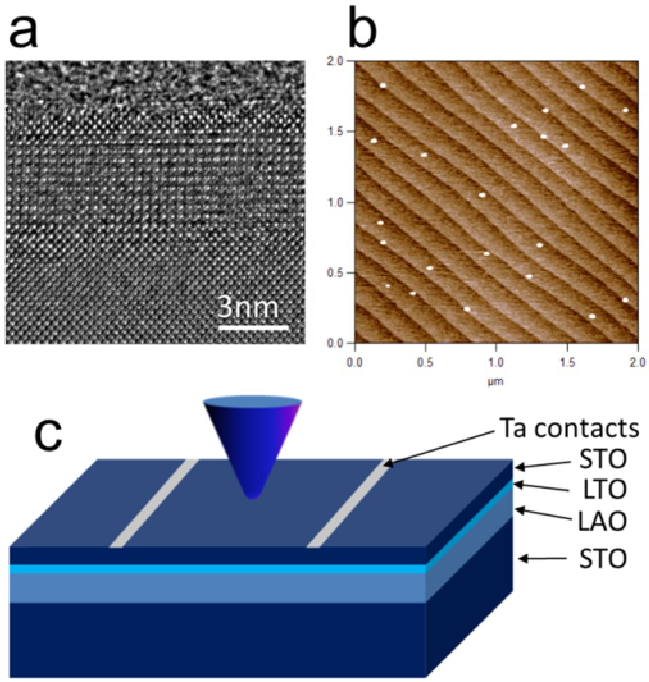

Altfeder et al. Figure 2

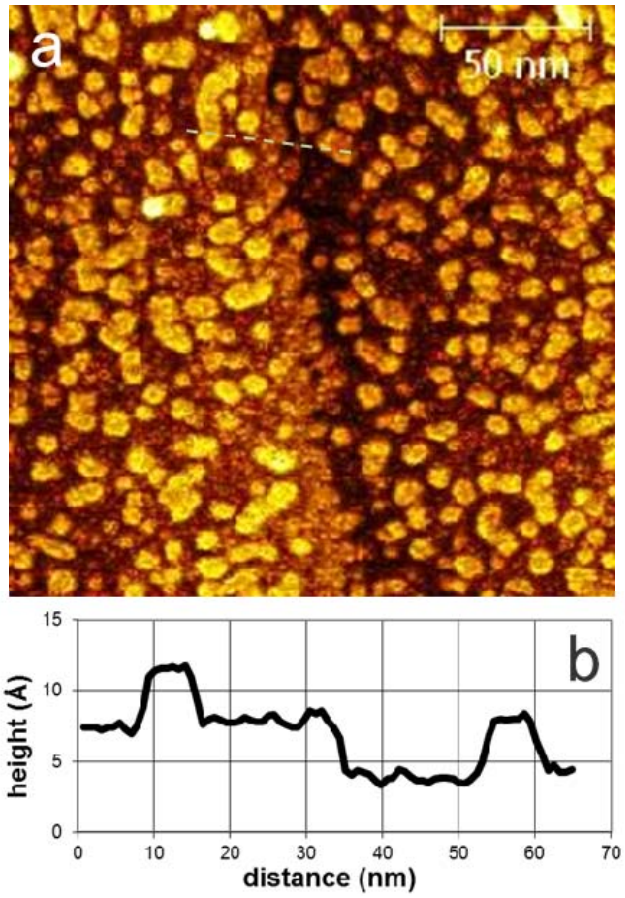

Altfeder et al. Figure 3

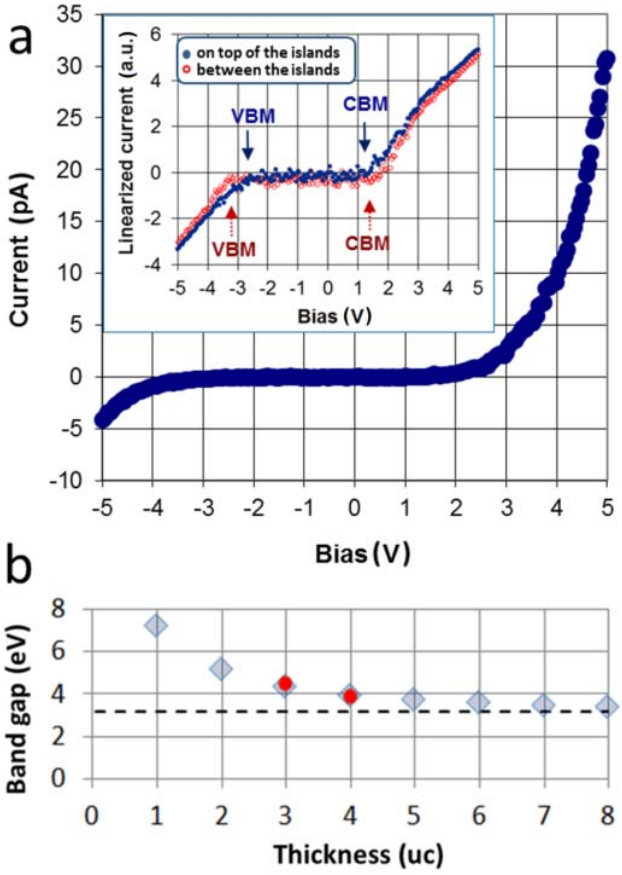

Altfeder et al. Figure 4

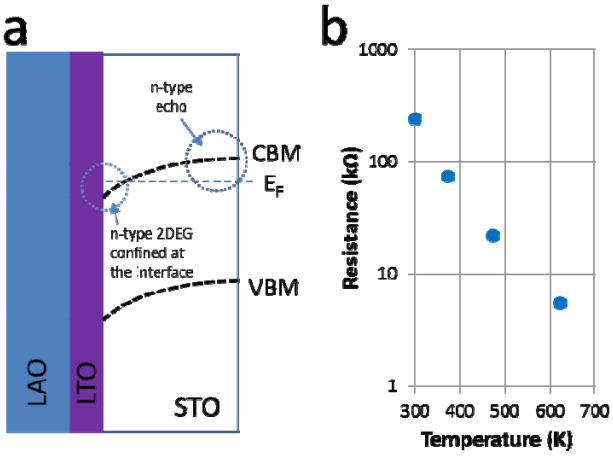

Altfeder et al. Figure 5